



Recognition of geochemical anomalies using a deep variational autoencoder network

Zijing Luo, Yihui Xiong, Renguang Zuo^{*}

State Key Laboratory of Geological Processes and Mineral Resources, China University of Geosciences, Wuhan, 430074, China



ARTICLE INFO

Editorial handling by Prof. M. Kersten

Keywords:

Geochemical mapping
Variational autoencoder network
Deep learning
Mineral exploration

ABSTRACT

Deep learning (DL) algorithms have received increased attention in various fields. In the field of geoscience, DL has been shown to be a powerful tool for mining complex, high-level, and non-linear geospatial data and for extracting previously unknown patterns related to geological processes. In this study, a deep variational autoencoder (VAE) network was used to extract features related to mineralization; and these features were then integrated as a anomaly map in support of mineral exploration based on geochemical exploration data, which consist of Cu, Pb, Mn, Zn and Fe₂O₃. Various experiments were conducted to determine the optimal parameters of the VAE. The structure of the VAE, in which the network depth and number of hidden units were 24–12–3–12–24, was built to recognize geochemical anomalies related to Fe polymetallic mineralization in the southwest Fujian Province, China. The geochemical anomalies recognized by the VAE show a close spatial correlation with known Fe polymetallic deposits. Meanwhile, the areas with high probability are located in or around the Yanshanian intrusions and the contact zones of the Carboniferous–Permian formation and Yanshanian intrusions. These results suggest that the anomalous areas identified by the VAE are meaningful for mineral exploration.

1. Introduction

Over the past several decades, geochemical anomalies have shown an increasingly important role in the field of geochemical prospecting (Caranza, 2008). The distribution of geochemical patterns is attributable to abundant primary and secondary geological processes, such as mineralization processes, which generally occur at different spatiotemporal scales, and interact with each other in complicated manners (Cheng, 2012; Wang and Zuo, 2020). Therefore, an effective separation of geochemical backgrounds from geochemical anomalies is a challenge owing to their complexity, nonlinearity, and variability (Goovaerts, 1997; Cheng, 2012), thus have attracted widespread attention in the field of exploration geochemistry (Cohen et al., 2010; Grunsky, 2010; Zuo and Wang, 2016; Zuo et al., 2016).

Methods for recognizing geochemical anomalies range from traditional frequency-based methods, such as mean \pm 2 standard deviations (Hawkes and Webb, 1962), probability graph (Sinclair, 1974), exploratory data analysis, for example, histograms and boxplots (Tukey, 1977; Kürzl, 1988), and multivariate statistics (Filzmoser et al., 2005; Yousefi et al., 2012, 2014), to frequency-spatial based methods, such as geo-statistics (Matheron, 1962) and fractal/multifractal models (Cheng

et al., 1994, 2000; Cheng, 2007; Zuo and Wang, 2016; Xiao et al., 2018, 2019, 2020). Recently, machine learning algorithms have received increased attention in geochemical anomaly recognition (e.g., Chen et al., 2014a; Xiong and Zuo, 2016; Mocini and Torab, 2017; Zhang et al., 2019; Yu et al., 2019; Zuo, 2017; Zuo et al., 2019; Chen et al., 2019; Zuo and Xiong, 2018, 2020). Owing to their ability to mining complex and high-level features from data (LeCun et al., 2015), machine learning algorithms have shown immense potential for complex and nonlinear geochemical data modeling (Xiong and Zuo, 2016; Zuo et al., 2019; Wang et al., 2020). Some supervised and unsupervised machine learning algorithms have been successfully adopted to quantify geochemical patterns related to mineralization. For example, supervised learning methods, including neural networks (Ziaii et al., 2009, 2012), metric learning (Wang et al., 2019a, 2019b), support vector machines (SVM) (Gonbadi et al., 2015), AdaBoost and random forest (Gonbadi et al., 2015), can be used to model labeled geochemical data and differentiate geochemical anomalies from the background. Unsupervised anomaly detection methods, such as one-class SVM (Chen and Wu, 2017), continuous restricted Boltzmann machine (Chen et al., 2014a) and isolation forest (Wu and Chen, 2018), have also been introduced for the recognition of geochemical anomalies in geochemistry exploration.

* Corresponding author.

E-mail address: zrguang@cug.edu.cn (R. Zuo).

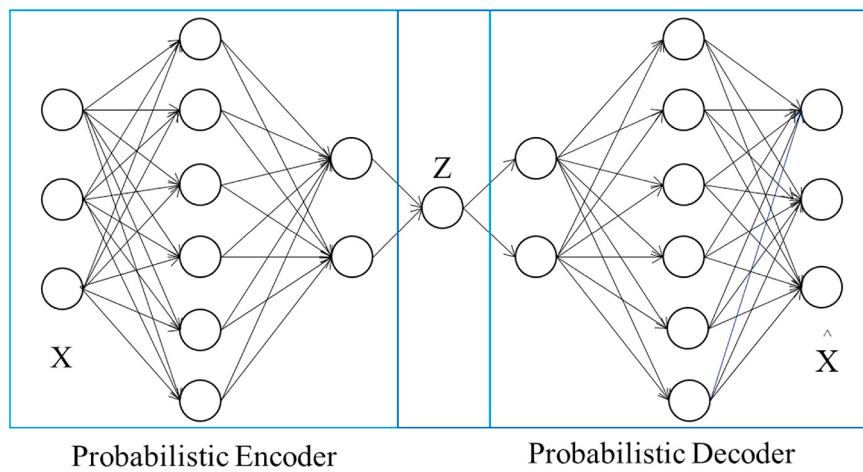


Fig. 1. An architecture of variational autoencoder network. For the meaning of each mathematical symbol, refer to the text.

As a subcategory of machine learning algorithms (Zhou et al., 2018), deep learning (DL) can learn features automatically from the data instead of applying a manual selection, improving the accuracy of the classification or prediction (She et al., 2018). In the field of geosciences, DL algorithms are widely used, such as hyperspectral image classification and anomaly detection (Chen et al., 2014b; Hu et al., 2015; Li et al., 2017), estimation of the arrival time of seismic waves (Ross et al., 2018), identification and classification of bad geological bodies (Chen et al., 2016), and denoising of seismic data (Han et al., 2018). DL algorithms such as deep autoencoder networks (Xiong and Zuo, 2016), convolutional autoencoder networks (Chen et al., 2019), and the hybrid method which integrates DL and classical anomaly detection methods (e.g., Xiong and Zuo, 2020; Wang et al., 2020; Zuo, 2020) have been applied for recognizing geochemical anomalies related to mineralization.

The deep autoencoder proposed by Hinton and Salakhutdinov (2006) is a type of artificial neural network, trained using unsupervised learning, and it has been applied to learn efficient coding (Gao et al., 2017). This autoencoder is trained to obtain a reconstruction of the input data in the output layer. The autoencoder generally consists of encoder part, which transforms the original input into a hidden layer representation through a deterministic mapping, and a decoder part, which remaps the hidden layer representation to the original input space through the same transformation (An and Cho, 2015). The difference between the original input and the reconstruction data is called reconstruction error. Xiong and Zuo (2016) used a deep autoencoder to extract geochemical anomalies according to the principle that the small probability samples (e.g. geochemical anomaly samples) have little contribution to the deep autoencoder network, thus corresponding to larger reconstruction errors.

Kingma and Welling (2013) proposed a variational autoencoder (VAE) (Fig. 1) to solve the problem in which the vector output of the hidden layer of the traditional autoencoder is chaotic and unknown. As a generation model, which is similar to a deep autoencoder architecture, VAE combines variational reasoning with deep learning, and better distributes the original data by assuming that the hidden layer variables follow Gaussian normal distribution (Cao et al., 2019). In recent years, the VAE which has been adopted for anomaly detection based on the reconstruction probability, which considers not only the differences between the data before and after reconstruction, but also the variance parameters of the distribution function to reconstruct the variability (An and Cho, 2015). In addition, the reconstruction probability solves the problem in that it is difficult to calculate the reconstruction error threshold when the input variables are heterogeneous data. VAE based anomaly detection with reconstruction probability is compared with other reconstruction-based methods such as principal component analysis (PCA) (An and Cho, 2015). The comparative results suggest that

VAE can obtain better results than PCA because PCA are not sufficient to capture the underlying structure of the data owing to its linear operations. In this study, the VAE was applied for recognizing geochemical anomalies associated with Fe polymetallic mineralization in the southwest Fujian Province, China, to verify its ability to deal with complex, high-level and non-linear multivariate geochemical patterns surveying for mineral exploration.

2. Methods

Compared with the low-dimensional embedding obtained by the autoencoder, the VAE network introduces a probabilistic perspective in the latent variable space, which can better describe the salient features of multivariate geochemical data. The fundamental purpose of the VAE is to use the latent variable z to characterize the distribution of the original data set $X = \{x_i\}_{i=1}^N$. We assume that the conditional distribution of the latent variable z is subject to a Gaussian distribution. The theory proves that the hidden variable z that satisfies the Gaussian distribution can generate data that satisfies any distribution through a neural network. By optimizing the generated parameter θ , the latent variable z generates a dataset $\hat{X} = \{\hat{x}_i\}_{i=1}^N$ that is highly similar to the original data $X = \{x_i\}_{i=1}^N$. This means that we will want to maximize the marginal likelihood $p_\theta(x)$ (Doersch, 2016):

$$p_\theta(x) = \int p_\theta(z)p_\theta(x|z)dz, \text{ with } z \sim N(0, I), \quad (1)$$

Because the real true posterior density $p_\theta(z|x)$ is intractable, to solve this problem, the VAE introduces a recognition model $q_\phi(z|x)$ to approximate the undetermined true posterior $p_\theta(z|x)$. The VAE measures the similarity between the recognition model $q_\phi(z|x)$ and true posterior distribution $p_\theta(z|x)$ using the Kullback-Leibler (KL) divergence.

$$\log p_\theta(x^{(i)}) = D_{KL}(q_\phi(z|x^{(i)}) || p_\theta(z|x^{(i)})) + L(\theta, \phi; x^{(i)}), \quad (2)$$

Because the KL divergence is always greater than 0, $\log p_\theta(x^{(i)}) \geq L(\theta, \phi; x^{(i)})$.

This formula $L(\theta, \phi; x^{(i)})$, called the (variational) lower bound on the marginal likelihood of data point i, can be expressed as follows:

$$L(\theta, \phi; x^{(i)}) = -D_{KL}(q_\phi(z|x^{(i)}) || p_\theta(z)) + E_{q_\phi(z|x^{(i)})} [\log p_\theta(x^{(i)}|z)], \quad (3)$$

To optimize $\log p_\theta(x)$, the variational lower bound on the marginal likelihood constitutes the overall optimization objective of the VAE. The first term on the right side of equation (3) equals the regularization term, and the second term is a negative reconstruction error in auto-encoder parlance. Therefore $q_\phi(z|x^{(i)})$ can be represented as a probabilistic

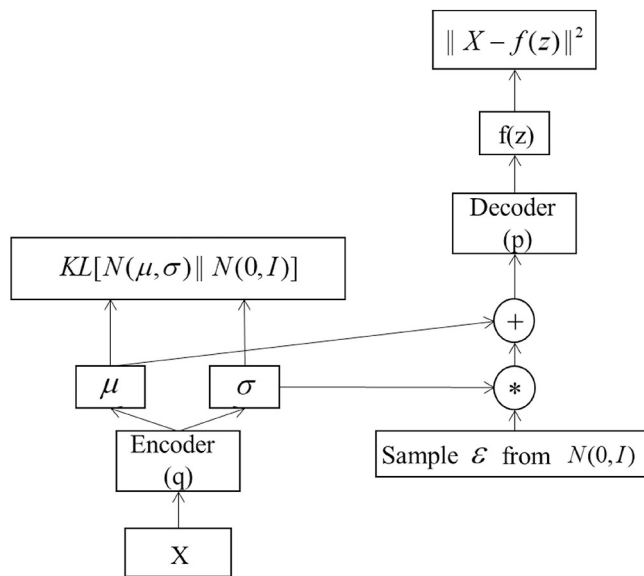


Fig. 2. Map of the reparameterization technique of variational autoencoder (modified from Doersch, 2016). For the meaning of each mathematical symbol, refer to the text.

encoder with a variational parameter ϕ , and $p_\theta(x^{(i)}|z)$ can be represented as a probabilistic decoder with a generation parameter of θ . The conditional distribution $p_\theta(x^{(i)}|z)$ is generally divided into two cases: a Bernoulli or Gaussian distribution (Doersch, 2016). In this study, because the input data of the network is multivariate geochemical data

rather than binary data, the distribution of $p_\theta(x^{(i)}|z)$ is assumed to be Gaussian.

Then, we calculate the stochastic gradient variational bayes estimator of the variational lower bound $L(\theta, \phi, x^{(i)})$. After introducing the recognition model $q_\phi(z|x^{(i)})$, we use the reparameterization technique (Fig. 2). Let z be a continuous random variable, and $z \sim q_\phi(z|x^{(i)})$ be a conditional distribution, with the introduction of an auxiliary noise variable $\epsilon \sim p(\epsilon)$. $p(\epsilon)$ has a known marginal likelihood distribution. Applying a distribution transformation on $q_\phi(z|x^{(i)})$ results in $\tilde{z} = g_\phi(\epsilon, x^{(i)})$. Because we assume that $q_\phi(z|x^{(i)})$ satisfies a Gaussian distribution, and that $p(z) = N(z; 0, I)$, when the approximation is $q_\phi(z|x^{(i)}) = N(z; u, \sigma^2 I)$, the regularization term is similar to the following:

$$-D_{KL}(q_\phi(z|x^{(i)})||p(z)) = \frac{1}{2} \sum_{j=1}^J (1 + \log(\sigma^{(i)2}) - u^{(i)2} - \sigma^{(i)2}), \quad (4)$$

where j is the dimension of z . When solving the reconstruction term, using a Monte Carlo evaluation, we obtain the following:

$$\mathbb{E}_{q_\phi(z|x^{(i)})} \left[\log p_\theta(x^{(i)}|z) \right] = \frac{1}{L} \sum_{l=1}^L \log(p(x^{(i)}|z^{(i,l)})), \quad (5)$$

According to the principle of the VAE, the data reconstruction can be deduced and the root cause of the exception can be analyzed (An and Cho, 2015).

In the training phase of the model, the entire model is trained with normal samples (non-deposits data). Thus, when the model receives a geochemical anomaly sample from the testing data, the encoder and decoder of the model will show larger reconstruction probability between the reconstructed data of the hidden variable z and the original

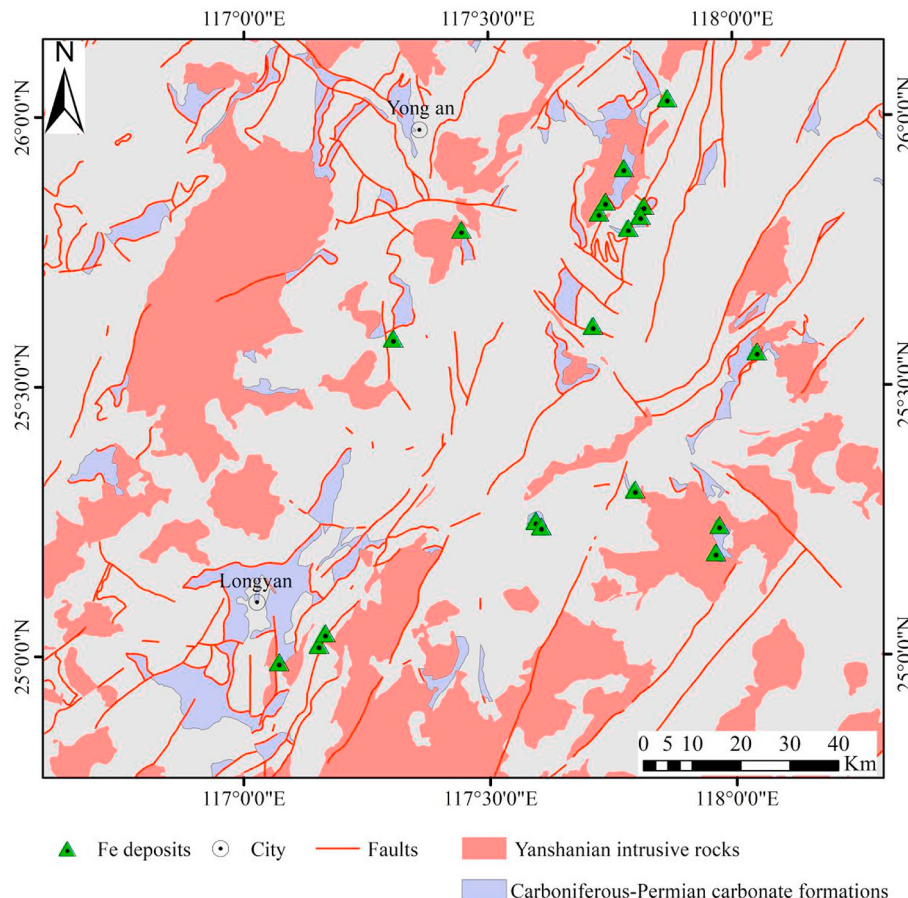


Fig. 3. Simplified geological map of Southwestern Fujian Province, China (after Xiong and Zuo, 2016).

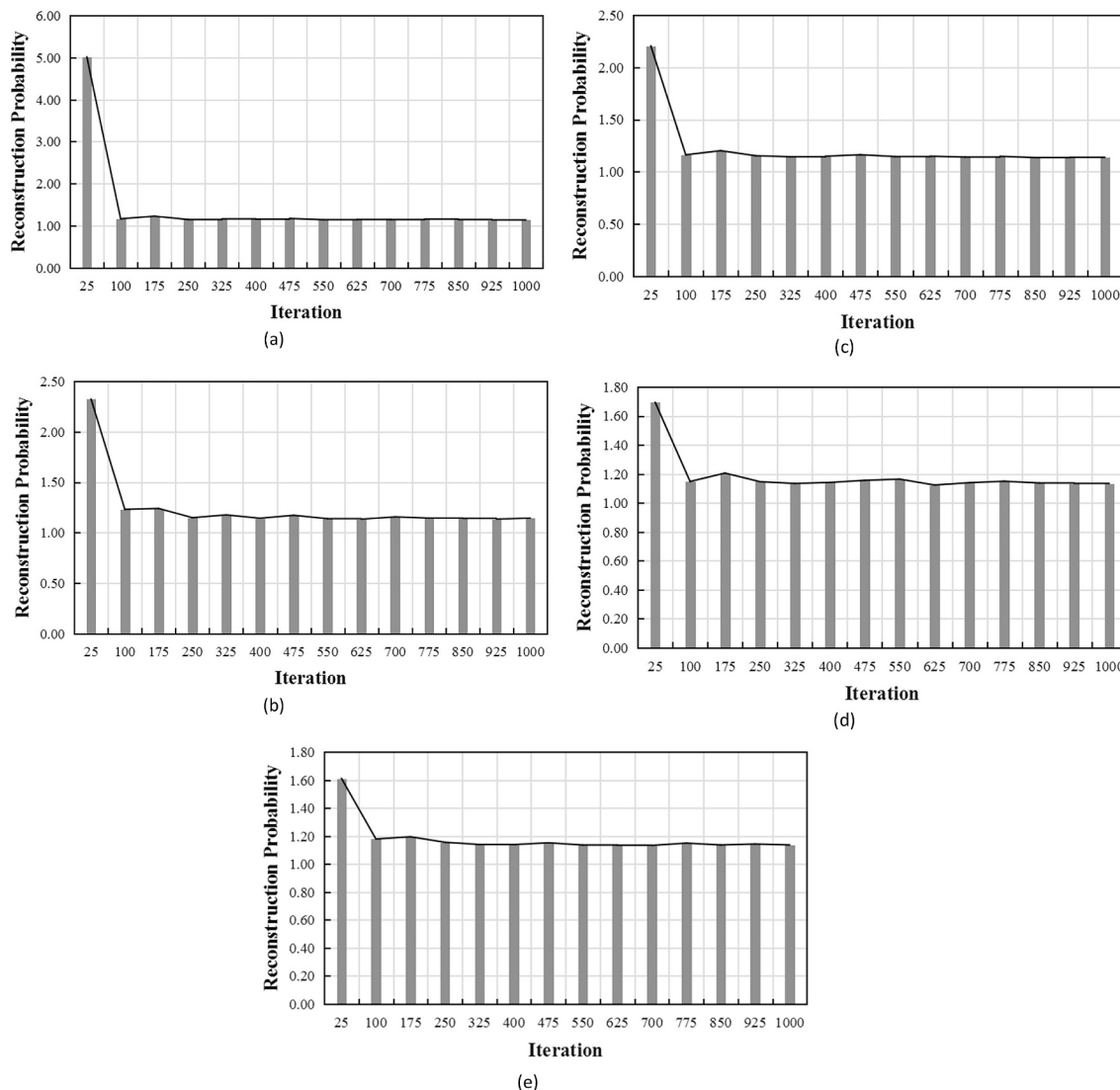


Fig. 4. Plot of training times versus. Reconstruction probability when the network depth is (a) 1-layer, (b) 2-layer, (c) 3-layer, (d) 4-layer, and (e) 5-layer.

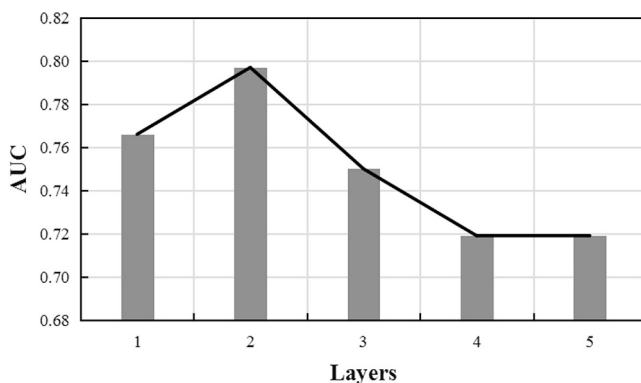


Fig. 5. AUC for different number of layers.

data.

3. Study area and data

The southwestern Fujian district (Fig. 3), located in Yangzte Block and Cathaysia Block, is well-known for the Mesozoic extensive

magmaism and numerous discovered Fe deposits (e.g. Makeng, Luoyang, Zhongjia and Dapai iron deposit) distributed along the early Hercynian Yong'an-Meixian fold belt above the Caledonian substrate (Ge et al., 1981). The geological evolution are multi-stage which consist of clastic and carbonate sedimentation, Indosinian W-E orogenic movement, the conversion of structure stress field of early Yanshanian, and extensive magmatism, and their corresponding evolution timing are late Devonian-Permian (D_3-P), Early-Middle Permian (T_1-T_2), Late Permian-Middle Jurassic (T_3-J_2) and Late Jurassic-Early Cretaceous (J_3-K_1), respectively (Zhou and Li, 2000; Sun et al., 2007). The ages of the granitoids determined through zircon U-Pb dating in Zhongjia, Dayang, Juzhou, Luoyang and Dapai are 99 Ma (Yang et al., 2008), 125–145 Ma (Zhang et al., 2012a; Wang et al., 2015), 132 Ma (Wang et al., 2015), 131–132 Ma (Zhang et al., 2012b) and 134 Ma (Yuan et al., 2013), respectively. The ages suggest that the Fe-related polymetallic mineralization exhibit a close temporal and spatial relationships with Yanshanian granites, acting as the heat and fluid source of mineralization. The three dominant faults, Zhenghe-Dapu, Nanping-Ninghua, and Shanghang-Yunxiao, combined with the widespread secondary faults are favorable channels for fluids flow (Zhang et al., 2015). The dominant lithologies and ore-hosting formations are the late Paleozoic marine sedimentary rocks and the middle-lower Carboniferous carbonate and clastic rock, respectively. Both of them can provide depositional space

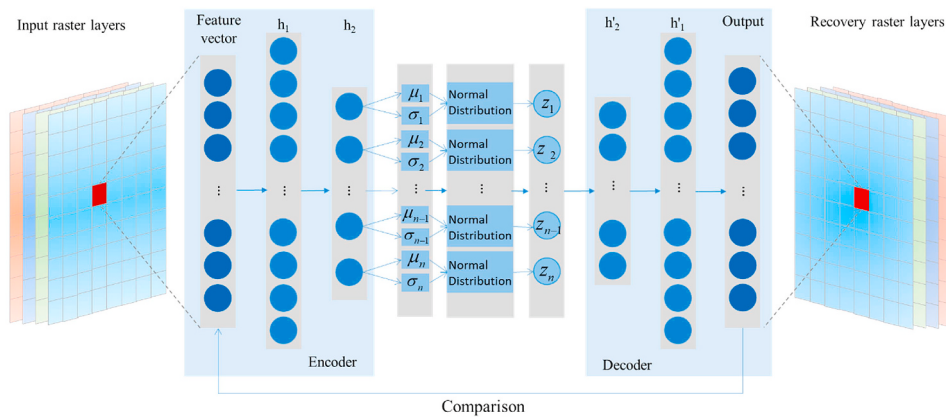


Fig. 6. Building and calculation process of VAE for anomaly detection (modified from Xiong and Zuo, 2016).

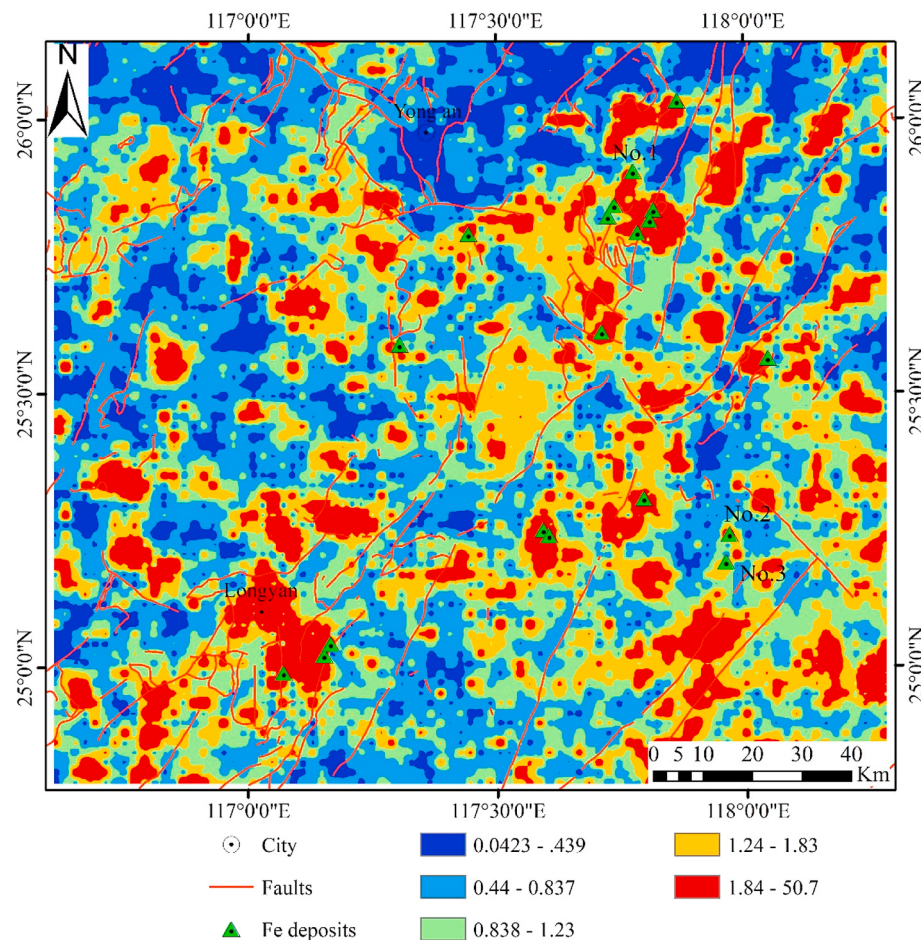


Fig. 7. Geochemical anomaly map obtained by the VAE.

for mineralization because their suitable physical/chemical condition for deposition (Zhang et al., 2015; Zuo et al., 2015).

In addition, skarn alterations, which are direct indicators for skarn-type deposits, can be reflected by geochemical anomalies recognized from exploration geochemical data. These data were collected at a 2 km × 2 km grid (Xie et al., 1997), and analyzed for 39 geochemical element concentrations. The analytical system of these 39 elements is introduced in detailed in Xie et al. (2008). Previous studies indicate that the skarn-type Fe deposits are closely related to the element association of Cu–Pb–Mn–Zn–Fe₂O₃ (Wang et al., 2015a, 2015b; Wang and Zuo, 2015; Xiong and Zuo, 2016). In this study, these five geochemical

elements were adopted for mining the statistical correlations between geochemical anomalies and known deposits. The geochemical data are typical compositional data, which involves the closure problem (Aitchison, 1986). Thus, the isometric logratio transformation (*ilr*) (Egozcue et al., 2003) was adopted to deal with the raw geochemical data prior to recognizing geochemical anomalies based on VAE. Here, the geochemical dataset was divided into approximately two parts in space, upper and lower, which were regarded as the training and testing datasets, respectively.

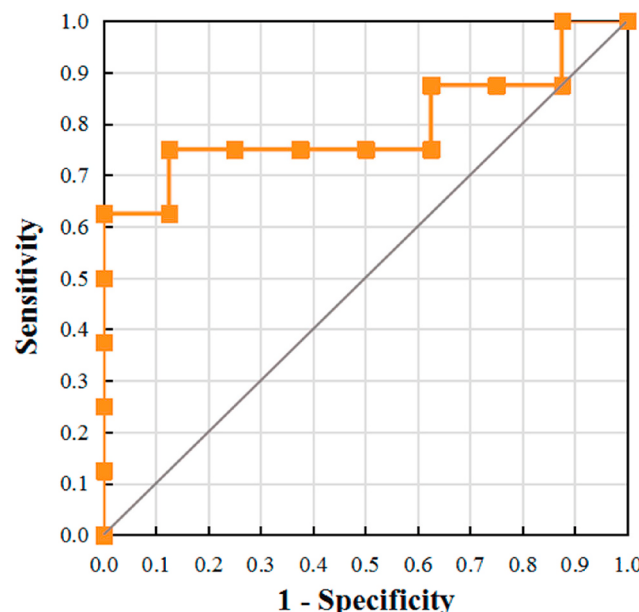


Fig. 8. AUC for the obtained pattern by the VAE.

4. Results and discussion

The anomaly detection task is carried out under the semi-supervised framework, and only a portion of the non-deposits data in the study area

is used to train the VAE. The probabilistic decoder outputs the mean and variance parameters for each sample from the probabilistic encoder. These parameters are used to calculate the probability of generating the original data from the distribution, and then regarding the probability as the anomaly score, which is called reconstruction probability (An and Cho, 2015).

The VAE network was built using a fully connected form based on the deep learning open source framework Tensorflow (<https://tensorflow.google.cn/>) and Python 3.5. In order to optimize the structure and anomaly detection ability of the VAE, various experiments were carried out to select the optimal VAE network parameters, such as optimization algorithm, network depth and the number of hidden units. According to the different dataset characteristics, different optimization algorithms can be selected, which possess different gradient update rules and gradient descent speeds. For convex optimization algorithms, such as the AdaGrad algorithm (Duchi et al., 2011), the scaling parameter is inversely proportional to the square root of the sum of all historical square values of the gradient. For non-convex optimization algorithms, such as the Adam algorithm (Kingma and Ba, 2014), use the first- and second-order moment estimations of the gradient to dynamically adjust the learning rate of each parameter. The gradient accumulation is an exponentially weighted moving average, and an offset correction is set to make the changes to the parameters relatively stable. The Adam algorithm is adopted in this study, the initial learning rate of which is set to 0.05. The number of trainings will affect the ability of the VAE network for anomalies detection. When the number of training times is too small, the data learned by the VAE network will be weak with poor judgment ability. When the training times are too many, the VAE network will tend to overfit, and a poor generalization ability may

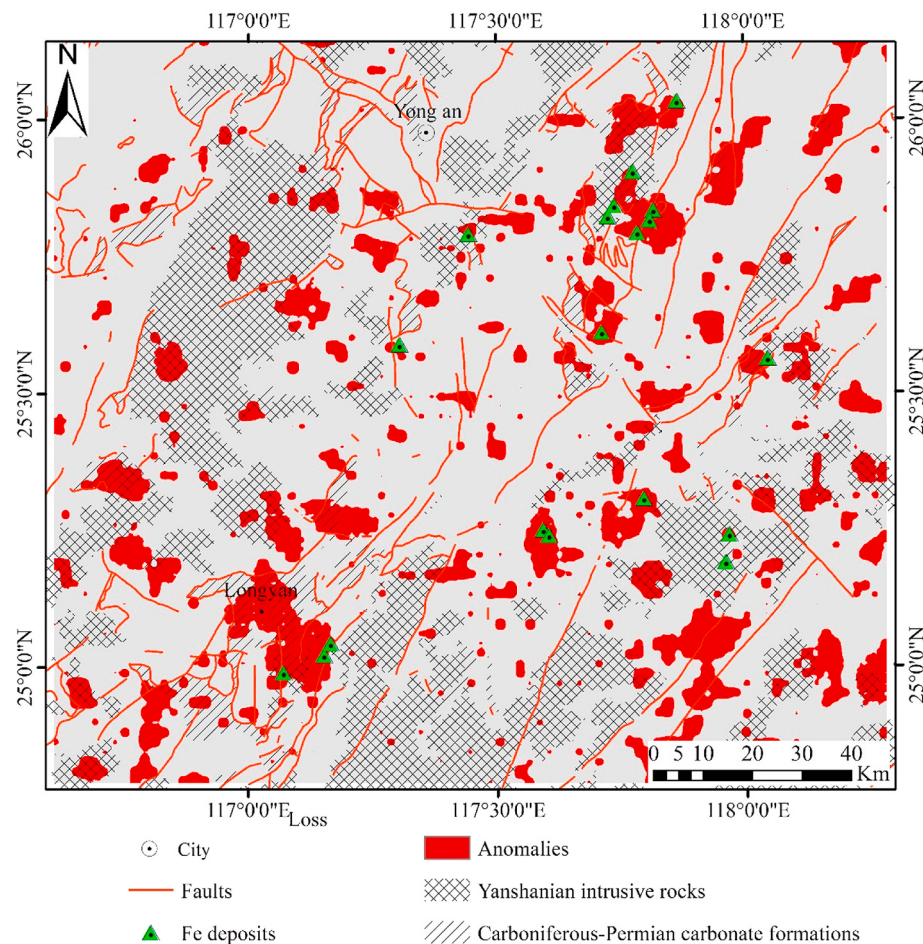


Fig. 9. The spatial relationship between high anomalies and geological factors.

occur. Therefore, it is necessary to obtain suitable training times through the relationship between the different training times and reconstruction probability. When the reconstruction probability becomes stable, the corresponding training number is considered to be optimal. The experimental results show that the network training is stable when the number of training times is 450 (Fig. 4).

A deeper network depth means a better non-linear expression ability, allowing of fitting more complex feature inputs, although the gradient instability brought about by a deep network will also cause network degradation problems, which will worsen the network performance. The comparative experiments with different network depths were conducted, and the corresponding receiver operating characteristic curve (Fawcett, 2006; Nykänen et al., 2015) and area under curve (AUC) value show that the network structure of 24–12–3–12–24 with the highest AUC (Fig. 5). The geochemical anomaly identification in the study area was performed by the VAE with the optimal parameters (Fig. 6). The mapped geochemical anomalies (Fig. 7) show that most of the known Fe polymetallic deposits occur in areas with a high anomaly probability. The geochemical anomalies recognized by the VAE show a close spatial correlation with the known Fe polymetallic mineralization, which is also indicated as an AUC value (0.797) of greater than 0.5 (Fig. 8).

Meanwhile, the area with a high probability is located in or around the Yanshanian intrusions, and in the contact zones of the C-P formation and Yanshanian intrusions (Fig. 9). Subsequently, the results were compared with the results of deep autoencoder (c.f., Fig. 8 in Xiong and Zuo, 2016). The extracted geochemical anomalies of these two architectures show similar spatial distribution patterns. However, by observing the spatial relationship between the mapped anomalies and known Fe polymetallic deposits, we find that the VAE can recognize the anomaly that the deep autoencoder cannot, such as the deposits numbered No.1, No.2 and No.3 (Fig. 7). This is mainly because the VAE based anomaly detection applies the reconstruction probability as anomaly scores, which considers both the differences between the reconstruction and the original input, and the variability of the reconstruction by considering the variance parameter of the distribution function. Variables with large variances can tolerate large differences in the reconstruction and the original data as a normal behavior while those with small variance can lower the reconstruction probability significantly. This is also a feature that the autoencoder lacks in due to its deterministic nature. Thus, VAE based on reconstruction probability has a stronger expressive power compared to the deep autoencoder in that even though normal and anomaly data might share the same mean value but with different variances. These observations suggest that the areas identified by the VAE are meaningful for mineral exploration, and the VAE is a powerful tool for processing geochemical exploration data.

5. Conclusions

In this study, an anomaly detection method using the reconstruction probability from the variational autoencoder was introduced to deal with geochemical exploration data. To illustrate the ability of VAE to quantify the large variability of the distribution of geochemical elements, the optimal network architecture of VAE optimized through trial and error training was used to identify multivariate geochemical anomalies associated with the Fe polymetallic mineralization in the southwestern Fujian district, China. The extracted anomalies have a high spatial correlation with the known Fe polymetallic deposits. The comparative study with deep autoencoder showed that VAE can recognize the anomalies that the deep autoencoder cannot. In addition, the obtained geochemical anomalies spatially coincide with the contact zones of the intrusions and C-P formation, which are favorable for locating the Fe polymetallic mineralization. These suggested that the reconstruction probability calculated by the stochastic latent variables that consider the parameters of the original input variable distribution are effective for recognizing geochemical anomalies, and can be used as an index for identifying geochemical anomalies.

Declaration of competing interest

The authors declare that they have no known competing financial interests or personal relationships that could have appeared to influence the work reported in this paper.

Acknowledgements

We thank three reviewers' comments and suggestions which help us improve this study. This study was supported by the National Natural Science Foundation of China (No. 41772344), and MOST Special Fund from the State Key Laboratory of Geological Processes and Mineral Resources, China University of Geosciences (MSFGPMR03-3).

References

- Aitchison, J., 1986. *The Statistical Analysis of Compositional Data*. Chapman & Hall, London, p. 416.
- An, J., Cho, S., 2015. Variational Autoencoder Based Anomaly Detection Using Reconstruction Probability. Special Lecture on IE, 2015, 2.
- Cao, W., Xu, J., Wang, J., 2019. Semi-supervised intrusion detection algorithm based on depth generation model. *Comput. Sci.* 46, 203–207 (In Chinese with English abstract).
- Carranza, E.J.M., 2008. *Geochemical Anomaly and Mineral Prospectivity Mapping in GIS*, vol. 11. Elsevier.
- Chen, G., An, k., Li, X., 2016. Identification and classification of bad geological bodies based on convolutional neural network. *Geol. Sci. Technol. Inf.* 35, 210–216.
- Chen, L., Guan, Q., Feng, B., Yue, H., Wang, J., Zhang, F., 2019. A multi-convolutional autoencoder approach to multivariate geochemical anomaly recognition. *Minerals* 9, 270.
- Chen, Y., Lu, L., Li, X., 2014a. Application of continuous restricted Boltzmann machine to identify multivariate geochemical anomaly. *J. Geochem. Explor.* 140, 56–63.
- Chen, Y., Lin, Z., Zhao, X., Wang, G., Gu, Y., 2014b. Deep learning-based classification of hyperspectral data. *IEEE J. Sel. Top. Appl. Earth Observ. Rem. Sens.* 7, 2094–2107.
- Chen, Y., Wu, W., 2017. Application of one-class support vector machine to quickly identify multivariate anomalies from geochemical exploration data. *Geochem. Explor. Environ. Anal.* 17, 231–238.
- Cheng, Q., 2007. Mapping singularities with stream sediment geochemical data for prediction of undiscovered mineral deposits in Gejiu, Yunnan Province, China. *Ore Geol. Rev.* 32, 314–324.
- Cheng, Q., 2012. Singularity theory and methods for mapping geochemical anomalies caused by buried sources and for predicting undiscovered mineral deposits in covered areas. *J. Geochem. Explor.* 122, 55–70.
- Cheng, Q., Agterberg, F.P., Ballantyne, S.B., 1994. The separation of geochemical anomalies from background by fractal methods. *J. Geochem. Explor.* 51, 109–130.
- Cheng, Q., Xu, Y., Grunsky, E., 2000. Integrated spatial and spectrum method for geochemical anomaly separation. *Nat. Resour. Res.* 9, 43–52.
- Cohen, D.R., Kelley, D.L., Anand, R., Coker, W.B., 2010. Major advances in exploration geochemistry, 1998–2007. *Geochem. Explor. Environ. Anal.* 10, 3–16.
- Doersch, C., 2016. Tutorial on Variational Autoencoders. 1606.05908.
- Duchi, J., Hazan, E., Singer, Y., 2011. Adaptive subgradient methods for online learning and stochastic optimization. *J. Mach. Learn. Res.* 12, 2121–2159.
- Egozcue, J.J., Pawlowsky-Glahn, V., Mateu-Figueras, G., Barcelo-Vidal, C., 2003. Isometric logratio transformations for compositional data analysis. *Math. Geol.* 35, 279–300.
- Fawcett, T., 2006. An introduction to ROC analysis. *Pattern Recogn. Lett.* 27, 861–874.
- Filzmoser, P., Garrett, R.G., Reimann, C., 2005. Multivariate outlier detection in exploration geochemistry. *Comput. Geosci.* 31, 579–587.
- Gao, N., Gao, L., He, Y., 2017. A lightweight intrusion detection model based on autoencoder network with feature reduction. *Acta Electron. Sin.* 45, 730–739.
- Ge, C., Han, F., Zhou, T., Chen, D., 1981. Geological characteristics of the Makeng iron deposit of marine volcano-sedimentary origin. *Acta Geosci. Sin.* 3, 47–69 (In Chinese with English Abstract).
- Goodbadji, A.M., Tabatabaei, S.H., Carranza, E.J.M., 2015. Supervised geochemical anomaly detection by pattern recognition. *J. Geochem. Explor.* 157, 81–91.
- Goovaerts, P., 1997. *Geostatistics for Natural Resources Evaluation*. Oxford University Press, p. 482pp.
- Grunsky, E.C., 2010. The interpretation of geochemical survey data. *Geochem. Explor. Environ. Anal.* 10, 27–74.
- Han, W., Zhou, Y., Chi, Y., 2018. Random noise removal of seismic data based on deep learning convolutional neural networks. *Geophys. Prospect. Pet.* 57, 72–79+87 (in Chinese with English abstract).
- Hawkes, H.E., Webb, J.S., 1962. *Geochemistry in Mineral Exploration*. Harper and Row, New York, p. 415.
- Hinton, G.E., Salakhutdinov, R.R., 2006. Reducing the dimensionality of data with neural networks. *Science* 313, 504–507.
- Hu, W., Huang, Y., Wei, L., Zhang, F., Li, H., 2015. Deep convolutional neural networks for hyperspectral image classification. *J. Sensors* 258619.
- Kingma, D.P., Ba, J., 2014. Adam: A Method for Stochastic Optimization. 1412.6980.
- Kingma, D.P., Welling, M., 2013. Auto-encoding Variational Bayes. 1312.6114.

- Kürzl, H., 1988. Exploratory data analysis: recent advances for the interpretation of geochemical data. *J. Geochim. Explor.* 30, 309–322.
- LeCun, Y., Bengio, Y., Hinton, G., 2015. Deep learning. *Nature* 521, 436.
- Li, W., Wu, G., Du, Q., 2017. Transferred deep learning for anomaly detection in hyperspectral imagery. *Geosci. Rem. Sens. Lett. IEEE* 14, 597–601.
- Matheron, G., 1962. Paris: Tome. *Traité de géostatistique appliquée*, vol. 1, p. 334. Editions Technip.
- Moeini, H., Torab, F.M., 2017. Comparing compositional multivariate outliers with autoencoder networks in anomaly detection at hamich exploration area, east of Iran. *J. Geochim. Explor.* 180, 15–23.
- Nykänen, V., Lahti, I., Niiranen, T., Korhonen, K., 2015. Receiver operating characteristics (ROC) as validation tool for prospectivity models-A magmatic Ni-Cu case study from the Central Lapland Greenstone Belt, Northern Finland. *Ore Geol. Rev.* 71, 853–860.
- Ross, Z.E., Meier, M.E., Hauksson, E., 2018. P wave arrival picking and first-motion polarity determination with deep learning. *J. Geophys. Res.* 123, 5120–5129.
- She, B., Tian, F., Liang, W., 2018. Fault diagnosis method based on deep convolution variational self-encoding network. *J. Instrum.* 10, 27–35.
- Sinclair, A., 1974. Selection of threshold values in geochemical data using probability graphs. *J. Geochim. Explor.* 3, 129–149.
- Sun, W., Ding, X., Hu, Y., Li, X., 2007. The golden transformation of the Cretaceous plate subduction in the west Pacific. *Earth Planet Sci. Lett.* 262, 533–542.
- Tukey, J.W., 1977. *Exploratory Data Analysis*. Addison-Wesley, Reading, USA.
- Wang, H., Cheng, Q., Zuo, R., 2015a. Quantifying the spatial characteristics of geochemical patterns via GIS-based geographically weighted statistics. *J. Geochim. Explor.* 157, 110–119.
- Wang, H., Cheng, Q., Zuo, R., 2015b. Spatial characteristics of geochemical patterns related to Fe mineralization in the southwestern Fujian province (China). *J. Geochim. Explor.* 148, 259–269.
- Wang, H., Zuo, R., 2015. A comparative study of trend surface analysis and spectrum-area multifractal model to identify geochemical anomalies. *J. Geochim. Explor.* 155, 84–90.
- Wang, S., Zhang, D., Vatuva, A., Yan, P., Ma, S., Feng, H., Yu, T., Bai, Y., Di, Y., 2015. Zircon U-Pb Geochronology, Geochemistry and Hf Isotope Compositions of the Dayang and Juzhou Granites in Longyan, Fujian and Their Geological Implications, vol. 44, pp. 450–468 (In Chinese with English abstract).
- Wang, Z., Dong, Y., Zuo, R., 2019a. Mapping geochemical anomalies related to Fe-polymetallic mineralization using the maximum margin metric learning method. *Ore Geol. Rev.* 107, 258–265.
- Wang, Z., Zuo, R., Dong, Y., 2019b. Mapping geochemical anomalies through integrating random forest and metric learning methods. *Nat. Resour. Res.* 28, 1285–1298.
- Wang, J., Zhou, Y., Xiao, F., 2020. Identification of multi-element geochemical anomalies using unsupervised machine learning algorithms: a case study from Ag-Pb-Zn deposits in north-western Zhejiang, China. *Appl. Geochem.* 104679.
- Wang, J., Zuo, R., 2020. Assessing geochemical anomalies using geographically weighted lasso. *Appl. Geochem.* 119, 104668.
- Wu, W., Chen, Y., 2018. Application of isolation forest to extract multivariate anomalies from geochemical exploration data. *Glob. Geol.* 21, 36–47.
- Xiao, F., Wang, K., Hou, W., Erten, O., 2020. Identifying geochemical anomaly through spatially anisotropic singularity mapping: a case study from silver-gold deposit in Pangxidong district, SE China. *J. Geochim. Explor.* 210, 106453.
- Xiao, F., Wang, K., Hou, W., Wang, Z., Zhou, Y., 2019. Prospectivity mapping for porphyry Cu-Mo mineralization in the Eastern Tianshan, Xinjiang, northwestern China. *Nat. Resour. Res.* 29, 89–113.
- Xiao, F., Chen, J., Hou, W., Wang, Z., Zhou, Y., Erten, O., 2018. A spatially weighted singularity mapping method applied to identify epithermal Ag and Pb-Zn polymetallic mineralization associated geochemical anomaly in Northwest Zhejiang, China. *J. Geochim. Explor.* 189, 122–137.
- Xie, X., Mu, X., Ren, T., 1997. Geochemical mapping in China. *J. Geochim. Explor.* 60, 99–113.
- Xie, X., Wang, X., Zhang, Q., Zhou, G., Cheng, H., Liu, D., Cheng, Z., Xu, S., 2008. Multiscale geochemical mapping in China. *Geochem. Explor. Environ. Anal.* 8, 333–341.
- Xiong, Y., Zuo, R., 2016. Recognition of geochemical anomalies using a deep autoencoder network. *Comput. Geosci.* 86, 75–82.
- Xiong, Y., Zuo, R., 2020. Recognizing multivariate geochemical anomalies for mineral exploration by combining deep learning and one-class support vector machine. *Comput. Geosci.* 140, 104484.
- Yang, Z., Zhang, D., Feng, C., She, H., Li, J., 2008. SHRIMP zircon U-Pb dating of quartz porphyry from Zhongjia Tin-polymetallic deposit in Longyan area, Fujian province, and its geological significance. *Miner. Deposits* 27, 329–335 (in Chinese with English abstract).
- Yu, X., Xiao, F., Zhou, Y., Wang, Y., Wang, K., 2019. Application of hierarchical clustering, singularity mapping, and Kohonen neural network to identify Ag-Au-Pb-Zn polymetallic mineralization associated geochemical anomaly in Pangxidong district. *J. Geochim. Explor.* 203, 87–95.
- Yousefi, M., Kamkar-Rouhani, A., Carranza, E.J.M., 2012. Geochemical mineralization probability index (GMPI): a new approach to generate enhanced stream sediment geochemical evidential map for increasing probability of success in mineral potential mapping. *J. Geochim. Explor.* 115, 24–35.
- Yousefi, M., Kamkar-Rouhani, A., Carranza, E.J.M., 2014. Application of staged factor analysis and logistic function to create a fuzzy stream sediment geochemical evidence layer for mineral prospectivity mapping. *Geochem. Explor. Environ. Anal.* 14, 45–58.
- Yuan, Y., Feng, H., Zhang, D., Di, Y., Wang, C., Ni, J., 2013. Geochronology of Dapai iron-polymetallic deposit in Yongding city, Fujian province and its geological significance. *Acta Mineral. Sin. (Suppl. I)*, 73–75 (in Chinese with English abstract).
- Zhang, C., Li, L., Zhang, C., Wang, J., 2012a. LA-ICP-MS zircon U-Pb ages and Hf isotopic compositions of Dayang granite from Longyan, Fujian province. *Geoscience* 26, 434–444 (in Chinese with English abstract).
- Zhang, D., Wu, G., Di, Y., Wang, C., Yao, J., Zhang, Y., Lv, L., Yuan, Y., Shi, J., 2012b. Geochronology of diagenesis and mineralization of the Luoyang iron deposit in Zhangping city, Fujian province and its geological significance. *J. China Univ. Geosci.* 37, 1217–1231 (in Chinese with English abstract).
- Zhang, S., Xiao, K., Carranza, E.J.M., Yang, F., Zhao, Z., 2019. Integration of auto-encoder network with density-based spatial clustering for geochemical anomaly detection for mineral exploration. *Comput. Geosci.* 130, 43–56.
- Zhang, Z., Zuo, R., Xiong, Y., 2015. A comparative study of fuzzy weights of evidence and random forests for mapping mineral prospectivity for skarn-type Fe deposits in the southwestern Fujian metallogenic belt, China. *Sci. China Earth Sci.* 59, 556–572.
- Zhou, X., Li, W., 2000. Origin of Late Mesozoic igneous rocks in Southeastern China: implications for lithosphere subduction and underplating of mafic magmas. *Tectonophysics* 326, 269–287.
- Zhou, Y., Wang, J., Zuo, R., Xiao, F., She, W., Wang, S., 2018. Machine learning, deep learning and Python language in field of geology. *Acta Petrol. Sin.* 34, 3173–3178.
- Ziaei, M., Pouyan, A.A., Ziae, M., 2009. Neuro-fuzzy modelling in mining geochemistry: identification of geochemical anomalies. *J. Geochim. Explor.* 100, 25–36.
- Ziaei, M., Ardejani, F.D., Ziae, M., Soleymani, A.A., 2012. Neuro-fuzzy modeling based genetic algorithms for identification of geochemical anomalies in mining geochemistry. *Appl. Geochem.* 27, 663–676.
- Zuo, R., 2017. Machine learning of mineralization-related geochemical anomalies: a review of potential methods. *Nat. Resour. Res.* 26, 457–464.
- Zuo, R., 2020. Geodata science-based mineral prospectivity mapping: a review. *Nat. Resour. Res.* <https://doi.org/10.1007/s11053-020-09700-9>.
- Zuo, R., Carranza, E.J.M., Wang, J., 2016. Spatial analysis and visualization of exploration geochemical data. *Earth Sci. Rev.* 158, 9–18.
- Zuo, R., Wang, J., 2016. Fractal/multifractal modeling of geochemical data: a review. *J. Geochim. Explor.* 164, 33–41.
- Zuo, R., Xiong, Y., 2018. Big data analytics of identifying geochemical anomalies supported by machine learning methods. *Nat. Resour. Res.* 27, 5–13.
- Zuo, R., Xiong, Y., 2020. Geodata science and geochemical mapping. *J. Geochim. Explor.* 209, 106431.
- Zuo, R., Zhang, Z., Zhang, D., Carranza, E.J.M., Wang, H., 2015. Evaluation of uncertainty in mineral prospectivity mapping due to missing evidence: a case study with skarn-type Fe deposits in Southwestern Fujian Province, China. *Ore Geol. Rev.* 71, 502–515.
- Zuo, R., Xiong, Y., Wang, J., Carranza, E.J.M., 2019. Deep learning and its application in geochemical mapping. *Earth Sci. Rev.* 192, 1–14.